blood®
Regular Article

PLATELETS AND THROMBOPOIESIS

Germline mutations in the transcription factor IKZF5 cause thrombocytopenia

Claire Lentaigne,[1-3,*] Daniel Greene,[3-5,*] Suthesh Sivapalaratnam,[3,6,*] Remi Favier,[7,8,*] Denis Seyres,[3,4,9] Chantal Thys,[10] Luigi Grassi,[3,4,9] Sarah Mangles,[11] Keith Sibson,[12] Matthew Stubbs,[1] Frances Burden,[3,4,9] Jean-Claude Bordet,[13] Corinne Armari-Alla,[14] Wendy Erber,[3,15,16] Samantha Farrow,[3,4,9] Nicholas Gleadall,[3,4] Keith Gomez,[17] Karyn Megy,[3,4,9] Sofia Papadia,[3,4,9] Christopher J. Penkett,[3,4,9] Matthew C. Sims,[3] Luca Stefanucci,[3,4] Jonathan C. Stephens,[3,4,9] Randy J. Read,[18] Kathleen E. Stirrups,[3,4,9] Willem H. Ouwehand,[3,4,9,19] Michael A. Laffan,[1,2] NIHR BioResource,[3] Mattia Frontini,[3,9,20] Kathleen Freson,[3,10,†] and Ernest Turro[3-5,9,†]

[1]Centre for Haematology, Hammersmith Campus, Imperial College Academic Health Sciences Centre, Imperial College London, London, United Kingdom; [2]Imperial College Healthcare National Health Service (NHS) Trust, London, United Kingdom; [3]National Institute for Health Research (NIHR) BioResource, Cambridge University Hospitals, Cambridge Biomedical Campus, Cambridge, United Kingdom; [4]Department of Haematology, University of Cambridge, Cambridge Biomedical Campus, Cambridge, United Kingdom; [5]Medical Research Council Biostatistics Unit, Cambridge Biomedical Campus, Cambridge, United Kingdom; [6]Department of Haematology, Barts Health National Health Service Trust, London, United Kingdom; [7]Assistance Publique–Hôpitaux de Paris, French Reference Center for Inherited Platelet Disorders, Armand Trousseau Children's Hospital, Paris, France; [8]INSERM UMR 1170, Gustave Roussy Institute, Villejuif, France; [9]NHS Blood and Transplant, Cambridge Biomedical Campus, Cambridge, United Kingdom; [10]Department of Cardiovascular Sciences, Center for Molecular and Vascular Biology, University of Leuven, Leuven, Belgium; [11]Department of Haematology, Hampshire Hospitals NHS Foundation Trust, Basingstoke, United Kingdom; [12]Haemophilia, Haemostasis and Thrombosis Centre, Great Ormond Street Hospital for Children National Health Service Trust, London, United Kingdom; [13]Hemostasis Laboratory, Biology Center, Hospices Civils de Lyon, Bron, France; [14]Paediatric Oncology Hematology Unit, Michalon Hospital, La Tronche, France; [15]School of Biomedical Science, University of Western Australia, Crawley, WA, Australia; [16]PathWest Laboratory Medicine, Nedlands, WA, Australia; [17]Katharine Dormandy Haemophilia Centre and Thrombosis Unit, The Royal Free Hospital, London, United Kingdom; [18]Department of Haematology, Cambridge Institute for Medical Research, University of Cambridge, Cambridge Biomedical Campus, Cambridge, United Kingdom; [19]Wellcome Sanger Institute, Wellcome Genome Campus, Hinxton, Cambridge, United Kingdom; and [20]British Heart Foundation Centre of Excellence, Cambridge Biomedical Campus, Cambridge, United Kingdom

KEY POINTS

- **Mutations in the transcription factor IKZF5 cause autosomal dominant thrombocytopenia and a paucity of α granules.**
- **Although *IKZF5* is expressed across hematopoietic lineages, misregulation in *IKZF5* cases is restricted to the megakaryocytic lineage.**

To identify novel causes of hereditary thrombocytopenia, we performed a genetic association analysis of whole-genome sequencing data from 13 037 individuals enrolled in the National Institute for Health Research (NIHR) BioResource, including 233 cases with isolated thrombocytopenia. We found an association between rare variants in the transcription factor-encoding gene *IKZF5* and thrombocytopenia. We report 5 causal missense variants in or near IKZF5 zinc fingers, of which 2 occurred de novo and 3 co-segregated in 3 pedigrees. A canonical DNA-zinc finger binding model predicts that 3 of the variants alter DNA recognition. Expression studies showed that chromatin binding was disrupted in mutant compared with wild-type IKZF5, and electron microscopy revealed a reduced quantity of α granules in normally sized platelets. Proplatelet formation was reduced in megakaryocytes from 7 cases relative to 6 controls. Comparison of RNA-sequencing data from platelets, monocytes, neutrophils, and CD4$^+$ T cells from 3 cases and 14 healthy controls showed 1194 differentially expressed genes in platelets but only 4 differentially expressed genes in each of the other blood cell types. In conclusion, IKZF5 is a novel transcriptional regulator of megakaryopoiesis and the eighth transcription factor associated with dominant thrombocytopenia in humans. (*Blood*. 2019;134(23):2070-2081)

Introduction

More than 30 genes have been implicated in hereditary thrombocytopenia,[1] of which 7 genes encode lineage-specific transcription factors (TFs).[2] Variants in 2 of these genes (*RUNX1* and *ETV6*) increase the risk of leukemia,[3,4] whereas others are associated with bone marrow failure (*HOXA11* and *MECOM*), red blood cell defects (*GATA1* and *GFI1B*), or syndromic disorders (*FLI1*).[5-8]

IKZF5 (Pegasus) is 1 of the 5 members of the Ikaros family of TF genes. *IKZF1* through *3* (Ikaros, Helios, and Aiolos), have established roles in lymphocyte development,[9] with germline mutations in *IKZF1* implicated in common variable immunodeficiency and somatic variants in both *IKZF1* and *IKZF3* associated with hematological malignancies.[10-12] In contrast, the functions of *IKZF4* (Eos) and *IKZF5*, which are both widely expressed in hematopoietic cells,[13] have remained unknown. *IKZF5* encodes a DNA-binding factor that recognizes elements containing the core sequence GNNTGTNG via its 3 N-terminal zinc fingers (Znfs), whereas the C-terminal Znfs control self-association of Ikaros proteins. IKZF5 is highly homologous to the other Ikaros

proteins except at the N terminus, where it contains 3 rather than 4 Znfs and has distinct DNA-binding sites.[14,15] Here, we present genetic and functional evidence demonstrating that rare missense variants in *IKZF5* cause thrombocytopenia.

Methods

Enrollment, research ethics, and consent

Enrollment of participants in the National Institute for Health Research (NIHR) BioResource–Rare Diseases occurred between December 2012 and March 2017. All participants provided written informed consent either under the East of England Cambridge South national research ethics committee reference 13/EE/0325 or alternate research ethics committee-approved studies for UK patients; obtaining consent for overseas samples was the responsibility of the respective principal investigator at the enrolling hospitals following oversight of the consent form for their study and a material transfer agreement.[16]

Clinical and laboratory phenotype data

We collected clinical data from probands and pedigree members and coded them with Human Phenotype Ontology terms as described previously.[17] Individuals with isolated thrombocytopenia were defined as those who had a Human Phenotype Ontology term "thrombocytopenia" or a platelet count (PLT) $<130 \times 10^9$/L and were deemed nonsyndromic (ie, did not have any severe abnormalities in other organ systems).

DNA sequencing and variant calling

DNA extraction, library preparation for whole-genome sequencing (WGS) and whole-exome sequencing (WES), variant calling, and variant annotation were performed as described previously.[16,17]

Variant confirmation and cosegregation studies

Variants called by WGS were confirmed and tested for in pedigree members by polymerase chain reaction (PCR) and Sanger sequencing. Primers were designed with Primer3Plus (https://primer3plus.com/cgi-bin/dev/primer3plus.cgi). Routine PCR was performed using MyTaq HS Mix (BIOLINE BIO-25045), a 2× Hot-start mix. Primers were used at a final concentration of 0.5 μM in 20-μL reactions. Thermal cycling using a Touchdown protocol,[18] with GeneAmp PCR System 9700 (Applied Biosystems, ThermoFisher). The Cycling protocol was an initial denature step of 3 minutes at 95°C, then 15 cycles of 95°C for 30 seconds, 70°C 1-minute touchdown (1°C/cycle), and 72°C for 30 seconds. The final cycling phase was 25 cycles of 95°C for 30 seconds, 55°C for 1 minute, and 72°C for 30 seconds, with a final extension of 72°C for 5 minutes. The PCR products were checked by agarose gel electrophoresis, column purified using QIAquick PCR Purification kit (QIAGEN catalog no. 28106) and eluted with 30 μL nuclease free water. The amplicons were quantified with QUBIT dsDNA BR assay kit (Life Technologies Ltd [Invitrogen Division] catalog no. Q32853). Purified, quantified amplicons were sent to Source Bioscience for Sanger sequencing, with the same primers that were used to amplify the target. The primers used were 5′-TCCAATGAATGGA CAAGCAA-3′ and 5′-TCGAGAGCTGATTCAAAGGG-3′, for variants at GRCh37 positions 10:124754093, 10:124754138, and 10:124754155, targeting a 530-bp amplicon. Variants called by WES were confirmed and tested for in pedigree members following a similar approach. The primers used were 5′-TTTTGTGAGAAGTGAACTGTC-3′ and 5′-AGGGCATC ACTTCTGACCTGT-3′, for variants at GRCh37 positions 10:124755560 and 10:124755540, targeting a 491-bp amplicon.

Genetic association analysis

We applied BeviMed[19] to compute a probability of association between each gene and case/control status, defined by presence or absence of isolated thrombocytopenia, among unrelated individuals, as described previously.[16] In general, we excluded somatic short variants/indels with an allele count in any GnomAD population in excess of what would be expected given a true population minor allele frequency of 1/10 000 (under a dominant model) or 1/1000 (under a recessive model).[16] Large deletions with an internal allele count among unrelated Europeans or non-Europeans in excess of what would be expected given a population allele frequency of 1/200 were also excluded.[16] To boost power, when assessing the evidence for genetic association with thrombocytopenia for a particular gene, cases with explanatory variants in other genes were treated as controls. Thus, the numbers of cases and controls varied slightly by gene, depending on whether the gene being assessed contained any cases carrying known pathogenic variants. Variant selection on the basis of allele frequency and predicted consequence was performed as described previously.[16] BeviMed compares the statistical support for a baseline model in which disease risk is independent of the genotypes with various association models in which disease risk depends on the allele configuration at the given rare variant sites, a latent partition of variants into pathogenic and benign groups, and a Mendelian mode of inheritance. The association models are fitted to different subsets of variants in a given locus corresponding to different predicted consequences, which imposes a prior correlation structure on the pathogenicity of the variants that reflects competing potential disease mechanisms.

Electron microscopy

We performed transmission electron microscopy (EM) analysis of platelets as described previously.[20] The platelet surface area (in square micrometers) and the number of α granules per unit area (in $1/\mu m^2$) were measured blinded to case/control status as done previously for *GATA1*- and *NBEAL2*-related granule defects.[21] Whole mount EM analysis to quantify dense granules was performed as described previously.[22]

Megakaryocyte differentiation assays

$CD34^+$ hematopoietic stem cells (HSCs) were isolated by magnetic cell sorting (Miltenyi Biotec, Bergisch Gladback, Germany) from peripheral blood. The recovered (differentiation day 0) $CD34^+$ HSCs were cultured in StemSpan SFEM medium with StemSpan CC100 ensuring expansion of HSC for 3 days (Stem Cell Technologies, Vancouver, Canada). Liquid megakaryocyte (MK) cultures were obtained by incubation with 50 ng/mL thrombopoietin, 25 ng/mL stem cell factor, and 10 ng/mL interleukin 1β (Peprotech, Rocky Hill, NJ). MKs were analyzed by flow cytometry on total differentiation day 10 for CD41 and CD42 markers. Proplatelet formation (PPF) was quantified after immunostaining of the cytoskeletal protein F-actin with phalloidin-rhodamine (Sigma, St Louis, MO) and α granule marker von Willebrand factor (VWF; A0082; Dako). For immunostaining, MKs were seeded for 4 hours on fibrinogen-coated coverslips to allow PPF; stained cells were photographed at 63× magnification with a confocal microscope (AxioObserver Z1; Zeiss, Heidelberg,

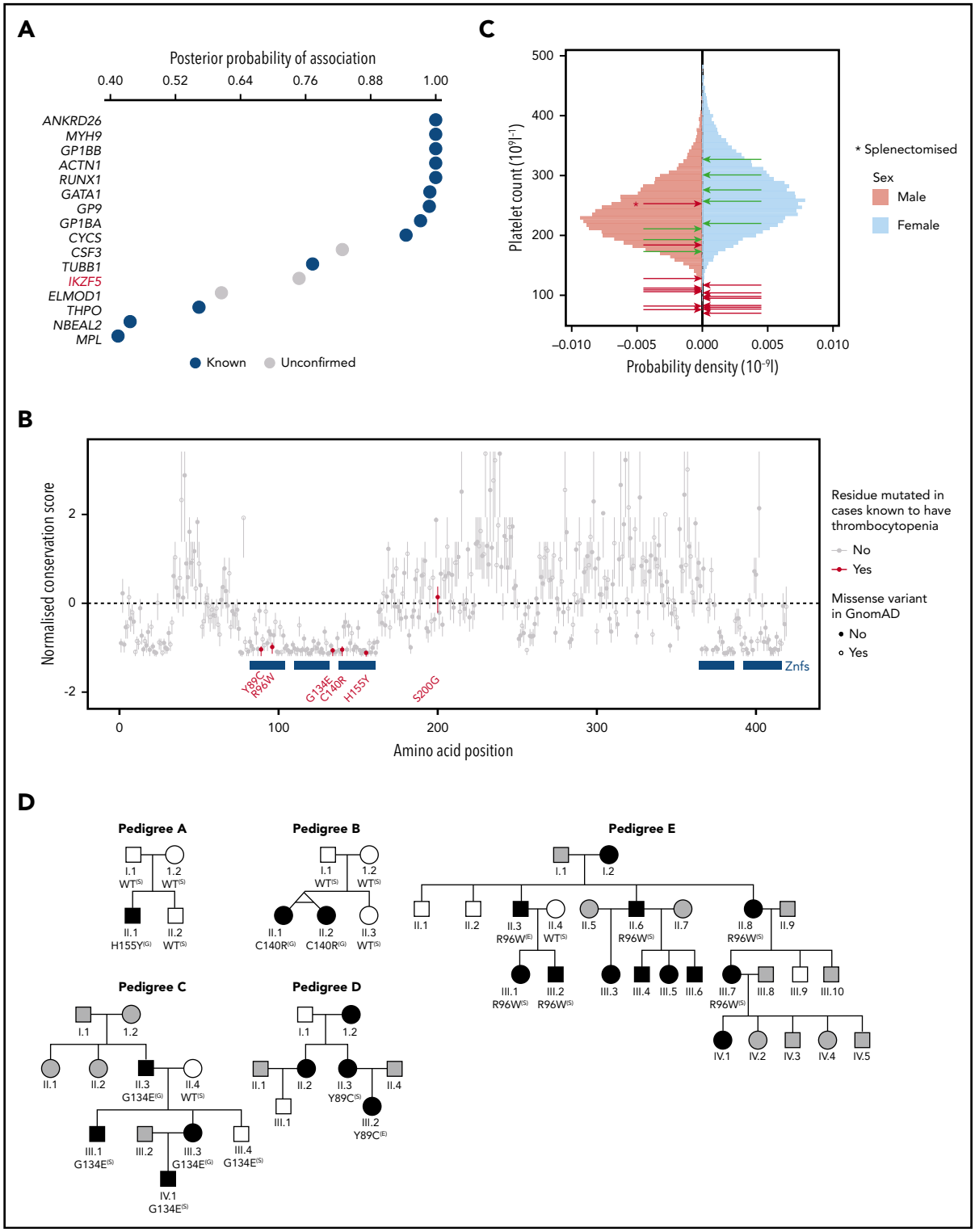

Figure 1. Rare missense variants in *IKZF5* are associated with thrombocytopenia. (A) BeviMed was applied gene by gene to infer associations between the genotypes of filtered rare variants and a case/control grouping defined by isolated thrombocytopenia. The posterior probabilities for genetic association inferred by BeviMed exceeding 0.4 are shown. The dots representing posterior probabilities for genes previously known to be implicated in hereditary thrombocytopenia are highlighted in blue. Genes not previously associated with thrombocytopenia are in gray. (B) Evolutionary conservation scores with respect to 66 protein sequences obtained using multiple sequence alignment within ConSurf,[31] and the corresponding 95% confidence intervals, for amino acids (AAs) 1 through 419 of IKZF5, normalized to have a mean of 0 and standard deviation of 1. The filled/empty points indicate presence/absence of missense variants in GnomAD altering the AAs. Only 3 of the 141 456 individuals in GnomAD harbor a missense variant affecting a residue in the N-terminal Znfs with a normalized conservation score <-1 (AAs 102, 111, and 123). The blue boxes indicate the locations of the Znfs. The variants in cases with thrombocytopenia affecting the 5 conserved AAs have been followed up in cosegregation studies, while S200G, which affects a non-conserved AA, has not been followed up. (C) Sex-stratified histograms of PLT obtained using a Sysmex hematology analyzer from 48 345 blood donors from the Efficiency and Safety of Varying the Frequency of Whole Blood Donation study[32] after adjustment for technical artifacts. The red arrows superimposed on the histograms indicate the sex of and values for cases carrying 1 of the 5 missense rare variants. The green arrows indicate the sex of and values for relatives homozygous for the corresponding WT allele. Individual C II.3, marked with

Germany). PPF of MKs was assessed by random imaging of 40 MKs per condition.

Structural modeling

We modeled the functional consequences of the *IKZF5* mutations using the structural coordinates of Znf 4 of CCCTC-binding factor (CTCF), the closest homolog of known structure to IKZF5 (PDB entry 5kkq). We did a BLAST search against the UniRef90 database[23] to find unique relatives for the sequence covering Znfs 1 to 3 of IKZF5 (residues 84-161). Structural consequences of the mutations of this region of IKZF5 were evaluated in the context of the closest homolog of known structure. We used CCP4mg software[24] to visualize the 3-dimensional structure of IKZF5 domains

HEK293 expression and localization studies

We cloned wild-type (WT) and mutant *IKZF5* in the pSecTag2/HygroA vector (Life Sciences) to transfect HEK293 cells. We prepared protein extracts 48 hours after transfection using the subcellular protein fractionation kit for cultured cells (Thermo Scientific) to isolate chromatin-bound proteins. We performed western blotting using the following antibodies: rabbit polyclonal anti-IKZF5 (Atlas), rabbit monoclonal anti-glyceraldehyde-3-phosphate dehydrogenase (clone 14C10; Cell Signaling) and goat polyclonal anti-Histone H3 or HIST3H3 (clone C16; Santa Cruz). We performed staining with the ECL detection reagent (Life Technologies) and imaged chemiluminescent blots with the ChemiDoc MP imager and the ImageLab software, version 4.1 (Bio-Rad). Transfected cells were analyzed with a confocal microscope (AxioObserver.Z1) and a structured illumination microscope (Elyra S.1; Zeiss) was used for z-stack images. Images were analyzed with ZEN Black (Zeiss).

RNA-sequencing study

For each studied individual, we separated peripheral blood mononuclear cells by gradient centrifugation (Percoll 1.078 g/mL) and isolated neutrophils from the pellet after double red blood cell lysis. Peripheral blood mononuclear cells were further separated into monocytes by $CD14^+$ selection (Miltenyi) and total CD4 (Stem Cell Technologies) from the CD14 column flow through. Platelets were isolated from platelet-rich plasma after leukocyte ($CD45^+$) depletion as described previously.[25] All protocols used are available at http://www.blueprint-epigenome.eu/. Purified cells were resuspended in Trizol, from which RNA was extracted following the manufacturer's instructions. For each cell type, reverse transcription and preparation of a high-throughput sequencing library was performed using the Riboerase Kapa stranded RNA kit following the manufacturer's instructions. We generated 150-bp paired-end reads on an Illumina Hiseq4000. We used TrimGalore, version 0.3.7 (http://www.bioinformatics.babraham.ac.uk/projects/trim_galore/), with parameters "-q 15 -s 3 -length 30 -e 0.05" to trim PCR and sequencing adapters. Trimmed reads were aligned to the Ensembl version 80[26] human transcriptome with Bowtie 1.0.1[27] using the parameters "-a -best -strata -S -m 100 -X 500 -chunkmbs 256 -nofw -fr." We used MMSEQ (version 1.0.8a)[28] with default parameters to quantify gene expression. We inferred differential expression using MMDIFF.[29] Genes with a posterior probability (PP) of differentially expression >0.8 were considered differentially expressed. We performed Reactome pathway enrichment analysis using the compareCluster and enrichPathway functions from the ReactomePA Bioconductor R package.[30]

Results

Genetic analysis highlights *IKZF5* as a candidate gene for isolated thrombocytopenia

Using the BeviMed method for genetic association,[19] for each gene we compared the genotypes at rare variant sites of up to 105 unrelated unexplained individuals having isolated thrombocytopenia (cases) with the genotypes of up to 10 053 unrelated individuals unaffected by thrombocytopenia or with thrombocytopenia caused by variants in other genes (controls) (see "Methods"). Of 33 814 genes assessed, 16 yielded a PP of association >0.4, of which 13 are established genes implicated in thrombocytopenia (Figure 1A). The associations for *CSF3* and *ELMOD1* were likely not causal because their high PPs depended on variants absent from affected relatives of thrombocytopenic carriers being pathogenic. The BeviMed association between thrombocytopenia and *IKZF5* was driven by 4 rare missense variants. We next reviewed an in-house dataset of 534 samples analyzed by WES from other individuals enrolled in the NIHR BioResource, and identified 2 additional thrombocytopenic cases carrying 2 different rare missense variants in *IKZF5*. All 6 missense variants were absent from gnomAD and 5 variants, encoding Y89C, R96W, G134E, C140R, and H155Y, were at evolutionarily conserved residues located in or near the N-terminal Znfs and were thus selected for further detailed analysis, while a sixth missense variant, affecting residue 200 (S200G), was expected to be benign because it was located far from Znfs and outside evolutionarily conserved regions (Figure 1B).

Cosegregation studies showed that H155Y and C140R, in pedigrees A and B, respectively (Figure 1D), occurred de novo, with the latter appearing in monozygotic twins. Cosegregation studies of G134E, Y89C, and R96W, in pedigrees C, D, and E, respectively, identified 10 additional relatives carrying mutant alleles and 2 unaffected relatives homozygous for the WT allele. Only 2 of the 10 individuals carrying the mutant allele had PLT $>150 \times 10^9$/L: a father and son in pedigree C. Case C II.3 was a 53-year-old male with a PLT in adulthood of 253×10^9/L who had undergone a splenectomy as a child for treatment of thrombocytopenia. One of his sons (C III.1) had a PLT level of 183×10^9/L, which is in the 11.6th percentile of the PLT distribution for healthy males[32] (Figure 1C; Table 1). Unfortunately, he was not available to obtain a second PLT measurement or for more detailed phenotyping. All other individuals who carried the mutant *IKZF5* allele across the 5 pedigrees had PLT $<150 \times 10^9$/L, with a normal platelet size (Table 1). Overall, 8 of 16 carriers

Figure 1 (continued) an asterisk, had thrombocytopenia as a child (with an unknown PLT) and was subsequently splenectomized, likely explaining why his PLT increased to 253×10^9/L as an adult. (D) The 5 pedigrees recalled for cosegregation. Male (square) and female (circle) individuals are shown in black or white depending on whether they are affected or unaffected, respectively, whereas individuals with an unknown PLT are shown in gray. Genotyping results obtained by WGS [(G)], WES [(E)], or Sanger sequencing [(S)] are shown in terms of their predicted amino acid substitutions underneath the genotyped individuals. Crl, control; WT, homozygous for the reference allele. C III.4 carries the G134E variant but has a PLT of 184.

Table 1. Information on pedigree members

Pedigree	ID	Sex	Genotype	Sequencing	TCP	PLT	MPV	BD	Blood film analysis	α granule quantity by EM	Immunoglobulins
A	I.1	M	WT	Sanger	N	211	11.4				
A	I.2	F	WT	Sanger	N	276	10.5				
A	II.1	M	H155Y het*	WGS	Y	76	10.2	None		Reduced	Normal
A	II.2	M	WT	Sanger	N	193	10.8				
B	I.1	M	WT	Sanger	N	173					
B	I.2	F	WT	Sanger	N	301					
B	II.1	F	C140R het*	WGS	Y	78	10.4	None	TCP, all else normal	Reduced	Normal
B	II.2	F	C140R het*	WGS	Y	83	10.2	None	TCP, all else normal	Reduced	Normal
B	II.3	F	WT	Sanger	N	257	10.9		Normal		
C	II.3	M	G134E het	WGS	N	253†	12.5				
C	II.4	F	WT	Sanger	N	327	11.4				
C	III.1	M	G134E het	Sanger	Y	128	9.4				
C	III.3	F	G134E het	WGS	Y	82	8.6	None	TCP, all else normal		
C	III.4	M	G134E het	Sanger	N	184	11.1				
C	IV.1	M	G134E het	Sanger	Y	82	8.8				
D	I.1	M			N						
D	I.2	F			Y						
D	II.2	F			Y	110	8.2				
D	II.3	F	Y89C het	Sanger	Y	97	8.9				Normal
D	III.1	M			N	195	9				
D	III.2	F	Y89C het	WES	Y	70	8.3				
E	I.2	F			Y						
E	II.1	M			N	255					
E	II.2	M			Y	155					
E	II.3	M	R96W het	WES	Y	107	9.5	None	Normal	Reduced	Normal
E	II.4	F	WT	Sanger	N	220	9				
E	II.6	M	R96W het	Sanger	Y	111	10.4	None	Normal	Reduced	Normal
E	II.8	F	R96W het	Sanger	Y	104	11	Mild	Normal	Reduced	Normal
E	III.1	F	R96W het	Sanger	Y	96	8.9	None			
E	III.2	M	R96W het	Sanger	Y	110	9.4	None			

Blank entries are not known/not applicable.

BD, bleeding diathesis (none/mild/severe); F, female; het: heterozygous; M, male; MPV, most recent mean platelet volume; N, no; PLT, the mean of PLT measurements is shown where multiple counts had been obtained; TCP, thrombocytopenia; WT: homozygous for the reference allele; Y, yes.

*de novo mutation.

†PLT measured only after splenectomy to correct thrombocytopenia.

Table 1. (continued)

Pedigree	ID	Sex	Genotype	Sequencing	TCP	PLT	MPV	BD	Blood film analysis	α granule quantity by EM	Immunoglobulins
E	III.3	F			Y	127	11				
E	III.4	M			Y	135	8.8				
E	III.5	F			Y	106	12				
E	III.6	M			Y	140	11.9				
E	III.7	F	R96W het	Sanger	Y	117	11.4	Mild	Normal	Reduced	Normal
E	III.9	M			N	275					
E	IV.1	F			Y	110					

Blank entries are not known/not applicable.

BD, bleeding diathesis (none/mild/severe); F, female; het: heterozygous; M, male; MPV, most recent mean platelet volume; N, no; PLT, the mean of PLT measurements is shown where multiple counts had been obtained; TCP, thrombocytopenia; WT: homozygous for the reference allele; Y, yes.

*de novo mutation.

†PLT measured only after splenectomy to correct thrombocytopenia.

(ie, 50%) had a PLT $<100 \times 10^9$/L and none had a PLT $<50 \times 10^9$/L. Because other members of the Ikaros family of Znf proteins are critical for lymphoid development and are associated with immune dysregulation and leukemia in humans, we specifically inquired about these features in the 5 pedigrees. No leukemias were reported in any of the pedigrees and there were no signs of immunodeficiency, such as recurrent infections. Immunoglobulin levels were normal in all cases for whom they were available (Table 1).

Platelets from *IKZF5* cases are depleted of α and dense granules and have an inconsistent aggregation defect

Imaging by light microscopy of blood smears from the probands of pedigrees A, B and E showed no structural abnormalities of platelets and no visible morphological defects in other blood cell types (Figure 2A; Table 1). Transmission EM analysis of platelets from 7 cases and 5 unrelated controls showed that, in keeping with previous measurements of mean platelet volume obtained by hematology analyzers, the platelet size distributions of the cases were normal (Figure 2B-C; Table 1). However, the platelets of the cases were significantly depleted of α granules (Figure 2B,D) and they had empty vacuoles and empty membrane structures (supplemental Figure 1, available on the *Blood* Web site). Whole mount EM analysis revealed a small but significant reduction in the number of dense granules per platelet in 2 cases from pedigree E (supplemental Figure 2). We performed platelet light transmission aggregometry (LTA) on the probands of pedigrees B, C, D and E. LTA was completely normal in the cases tested in pedigrees B and C but reduced in response to all agonists in the probands of pedigrees D and E (supplemental Table 1). 2 cases in pedigree E described mild bleeding symptoms but there was no significant bleeding history in any other cases (Table 1). Pregnancies had occurred in 5 cases resulting in 11 vaginal deliveries. No one required platelet supplementation during pregnancy or delivery, although 1 case (E II.8) required red cell transfusion for a postpartum hemorrhage in 1 out of 3 deliveries (Table 1; supplemental Table 2).

Structural modeling of *IKZF5* mutations

Although a crystal structure for IKZF5 (Pegasus) does not exist, the sequence covering Znfs 4 through 7 of the human CCCTC-binding factor CTCF[33] is 45% identical to IKZF5 over the 78 residues from C84 to H161 and contains no insertions or deletions. The relevant part of the bound DNA sequence in this structure, AGCAGGGGGC, conforms to the pattern identified for sequences bound by the IKZF5/Pegasus family, nGnnGnnnGn,[14] so similar interactions with DNA are expected to be conserved. We found a clear structural explanation for deleterious effects for 3 of the 5 mutations: Y89C would disrupt a binding contact with a backbone phosphate of the DNA; C140R would remove the first ligand in the third Znf domain; and R96W would disrupt a direct interaction with the penultimate guanine base of the consensus sequence in the major groove (Figure 3A). G134 is part of the most common consensus linker sequence between consecutive Znfs (TGEKP[35]) and it may play a role in flexibility during DNA recognition[36] and as a recognition site for threonine (or serine) phosphorylation during mitosis,[37] so mutations here would be expected to alter function. Although the structure of CTCF reveals no obvious reasons why H155Y could not be accommodated, the surrounding sequence SHHRRR is conserved in almost all of the top 50 hits from our BLAST[38] search, but is replaced by KMHILQ in CTCF, which suggests that H155 may be important for interaction with the remainder of IKZF5 or its binding partners. Our modeling thus predicted alterations in Znf binding to DNA for at least 3 of the variants, and we therefore expected alterations in cellular localization of IKZF5 in some of the mutants.

Abnormal nuclear localization and chromatin binding in *IKZF5* cases

To further investigate the effect of the *IKZF5* variants on DNA binding, we expressed the 5 causal mutants, the variant encoding S200G, a low-frequency variant (175 mutant alleles out of 280 830 in gnomAD) encoding I98V in the third Znf domain and WT IKZF5 in HEK293 cells, which do not express this TF. In contrast to WT IKZF5, which enters the nucleus to bind to

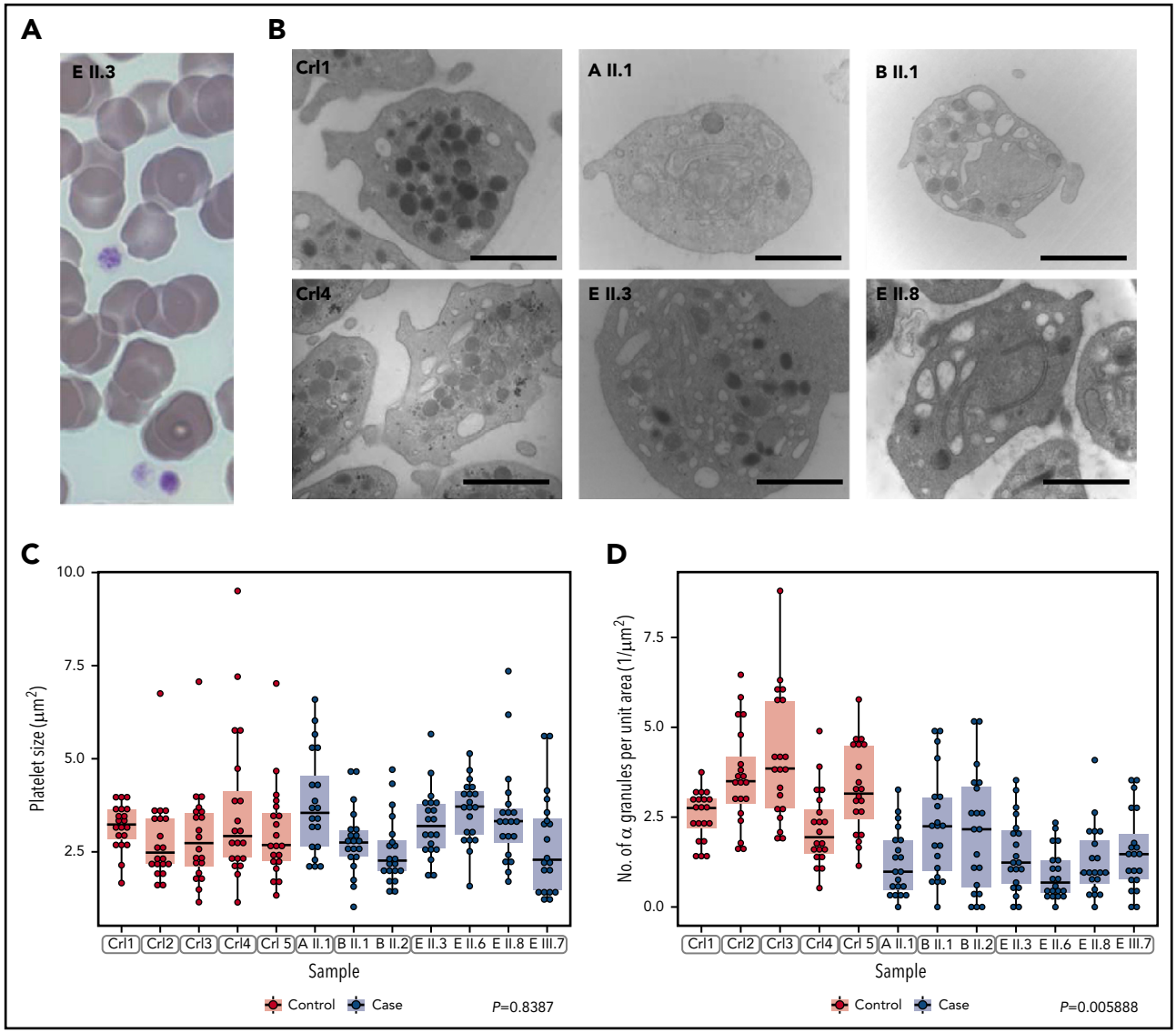

Figure 2. Cases have normally sized platelets but reduced numbers of α granules. (A) Representative May-Grünwald-Giemsa stained peripheral blood smear of patient E II.3. Platelets have a normal appearance (size and granularity) by light microscopy (magnification ×100). (B) Representative EM images for 2 unrelated healthy controls and 4 patients from pedigrees A, B, and E showing depletion of α granules. Marker is 1.5 μM for magnification x20 000. (C, D) The sizes and quantities of α granules per unit area of 20 platelets, quantified blinded to case/control status, in each of 5 cases and 7 controls. Linear mixed model with a fixed effect for case/control status, a random effect for pedigree (groupings in gray) and a random effect for sample. The *P* value under the null hypothesis that the fixed effect is equal to 0 is shown for each of the 2 responses.

chromatin, all 5 causal mutants exhibited a strong reduction in chromatin binding (Figure 3B-D), remaining instead in the cytosol and soluble membranes fractions (supplemental Figures 3 and 4). However, S200G and I98V entered the nucleus in a similar manner to WT IKZF5, suggesting that only missense substitutions of highly conserved residues in the N-terminal Znfs may cause thrombocytopenia (Figure 3B-C; supplemental Figure 3).

IKZF5 cases have abnormal PPF

Modeling and cellular localization studies of *IKZF5* mutants pointed to defective transcriptional regulation. Because thrombocytopenia can be caused by alterations of TF activity during megakaryopoiesis, we studied MK development in *IKZF5* cases. Microscopic evaluation of bone marrow aspirate smears from B II.2, D III.3, E II.8, and E III.2 showed a normal number of MKs without dysmegakaryopoiesis, which suggests normal maturation and differentiation of the megakaryocytic lineage. No abnormalities were present in the other lineages. We further studied MK development using blood-derived HSCs. MK differentiation evaluated by quantifying $CD41^+$ and $CD42b^+$ cells was comparable between subject E II.3 and 2 unrelated controls (Figure 4A). However, PPF by MK in these cultures seemed reduced for E II.3 compared with controls (Figure 4B). To further characterize the PPF defect, we quantified PPF after MK spreading on fibrinogen and staining with VWF and found it to be significantly reduced in 7 cases from 3 pedigrees compared with 6 unrelated healthy controls ($P = .0069$, linear mixed regression model; Figure 4C). However, there was no discernible difference in the number or spatial distribution of VWF^+ α granules in the MKs of cases compared with controls (supplemental Figure 5).

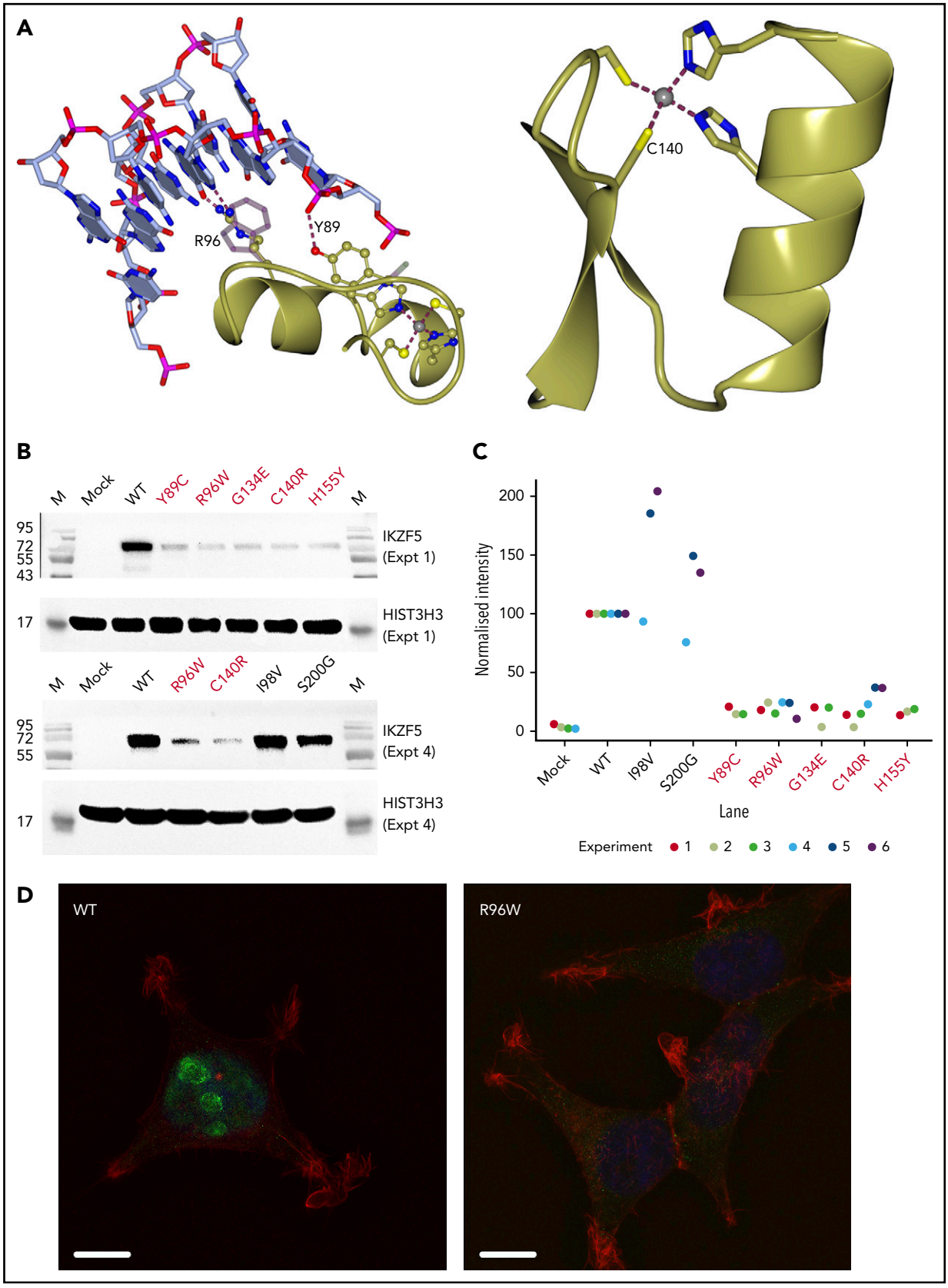

Figure 3. Structural modeling of the variants and expression studies in HEK293 cells. (A) Left panel: Mutation sites in Znf 1 of IKZF5. The structure of Znf 4 from CTCF (PDB entry 5kkq[33]) is portrayed as a template to understand the effect of the mutations Y89C (site equivalent to Y358) and R96W (site equivalent to K365). To model the conformation of R96, K365 in the CTCF structure was replaced by an arginine in a similar conformation to that of R369 in PDB entry 5kl6.[34] WT side chains are shown in ball-and-stick representation, whereas the mutated side chains are shown as partially transparent cylinders. Right panel: The role of C140 in Znf 3. We used the coordinates for Znf 6 from PDB entry

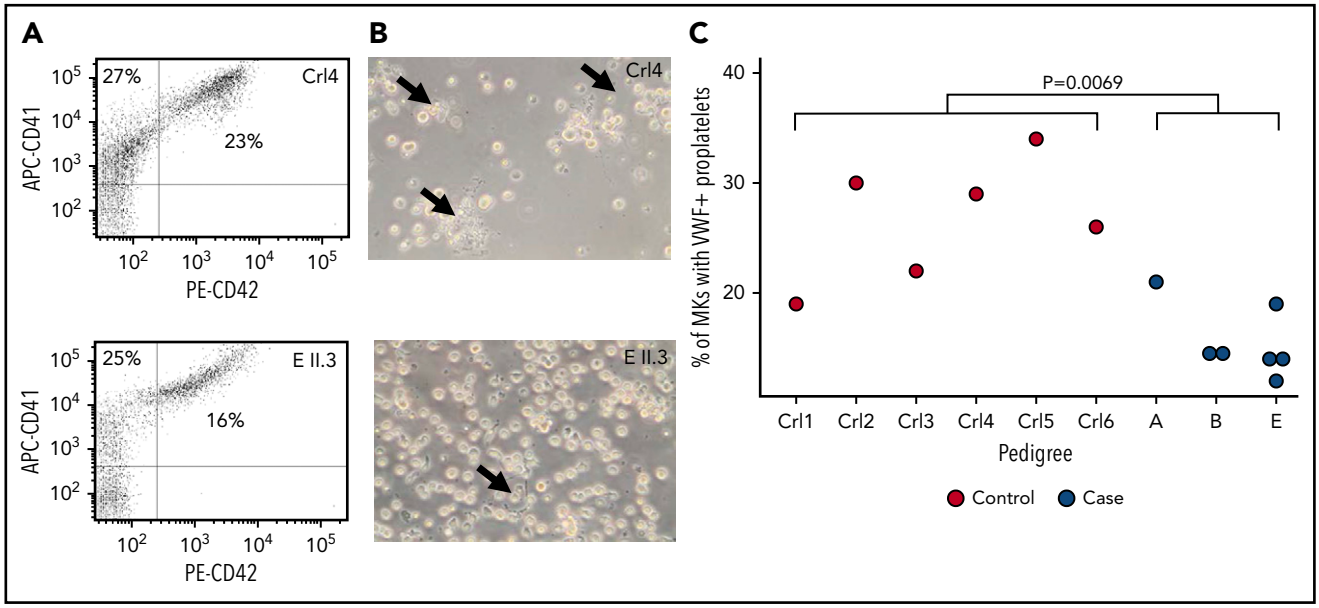

Figure 4. Reduced PPF in MKs from cases. (A) Flow cytometry analysis of day 10 MK for markers CD41 and CD42 showed no difference in maturation between control and case MKs. (B) The same cultures showed evidence of reduced PPF (arrows). (C) PPF was quantified after MK spreading on fibrinogen and staining for VWF for 6 unrelated controls and 7 cases. Linear mixed model with a fixed effect for case/control status, a random effect for pedigree and a random effect for sample. The *P* value under the null hypothesis in which that the fixed effect is equal to 0 is shown.

MK-specific transcriptional regulation if *IKZF5*

IKZF5 is expressed across hematopoietic lineages but *IKZF5* cases have normal blood counts, except for thrombocytopenia. To understand this, we performed RNA-sequencing on the $CD4^+$ T cells, monocytes, neutrophils, and platelets in 3 unrelated cases from pedigrees A, B, and E and 14 unrelated controls. We generated a mean of 51.3M paired-end reads per sample (range, 24.2M-83.9M), of which we aligned a mean of 29.4M (range, 15.4M-53.1M) to the reference human transcriptome (supplemental Figure 6). Our analysis revealed striking differences in the platelet transcriptome landscape only: 1194 protein-coding genes of 10 237 genes in Reactome[39] were differentially expressed in platelets but only 4 such genes were differentially expressed in each of the 3 other cell types (Figure 5A). The 631 downregulated, differentially expressed genes (DEGs) in platelets were significantly enriched for pathways involved in platelet function, hemostasis, and membrane and vesicle-mediated transport (Figure 5B), whereas upregulated DEGs had more general functions (supplemental Table 3). The most significantly enriched pathway among the downregulated DEGs was platelet activation, signaling and aggregation, for which 52 of 262 (19.8%) genes were significantly downregulated, including known disease-associated genes[2] involved in platelet formation (*CDC42*, *GP1BA*, *GP9*, *MPIG6B*) and function (*FERMT3*, *PLA2G4A*, *P2RY12*, and *TBXA2R*) (Figure 5C).

Discussion

Rare variants in other genes cause a combination of thrombocytopenia and α granule abnormalities. Rare variants in *NBEAL2* can cause Gray platelet syndrome (GPS), an autosomal recessive disease hallmarked by a complete absence of α granules and an enlargement of platelets, in addition to thrombocytopenia.[40,41] In the TF domain, *GATA1* mutations cause a paucity of α granules numbers and enlarged platelets,[21] *GFI1B* mutations cause a paucity of α granules and enlarged platelets,[42] *FLI1* mutations cause fused and enlarged α granules[43] and *RUNX1* mutations cause α granule storage and secretion defects.[44] Interestingly, our RNA-sequencing analysis from platelets lacking functional IKZF5 identified a striking platelet-specific defect, which is consistent with the isolated thrombocytopenia seen in the affected cases. Given the apparent lack of abnormalities in any cell types other than platelets, this may be the first TF-associated thrombocytopenia, which is completely lineage specific.

Transcriptome analysis identified hundreds of DEGs related to membrane and vesicle-mediated transport pathways, pointing to a possible mechanism for the α granule defect. *IKZF5*-related disorder does not appear to lead to a significant platelet function defect, as shown by the lack of bleeding symptoms in the majority of cases. Platelet function results obtained by light transmission aggregometry were inconsistent among the cases, with some having normal responses to all agonists. This variability is similar to that seen in other α granule defects such as GPS[45]; however, further studies of platelet function are required to understand the clinical implication, if any, of the observed paucity of α granules. In contrast to GPS, there was no clinical evidence of myelofibrosis (such as splenomegaly, other

Figure 3 (continued) 5kkq without any changes as all the side-chains shown are conserved between the 2 sequences. (B) Western blot analysis of HEK293 transfected cells with myc-tagged IKZF5 WT and mutants after extraction of chromatin-bound proteins. HIST3H3 (histone H3) serves as loading control. HEK293 transfected with empty vector (Mock) express no IKZF5. The 5 causal mutants are highlighted in red. (C) Quantification of chromatin-bound IKZF5 after transfections and normalization against HIST3H3. The 5 causal mutants are highlighted in red. (D) Immunofluorescence (z-stack images by a structured illumination microscope) using an antibody against IKZF5 (green), phalloidin (actin; red), and 4′,6-diamidino-2-phenylindole (nucleus, blue) showing punctate, nuclear staining for WT IKZF5, whereas R96W and other mutants (supplemental Figure 4) remain largely outside the nucleus after transfecting HEK293 cells. Scale bar, 10 μm.

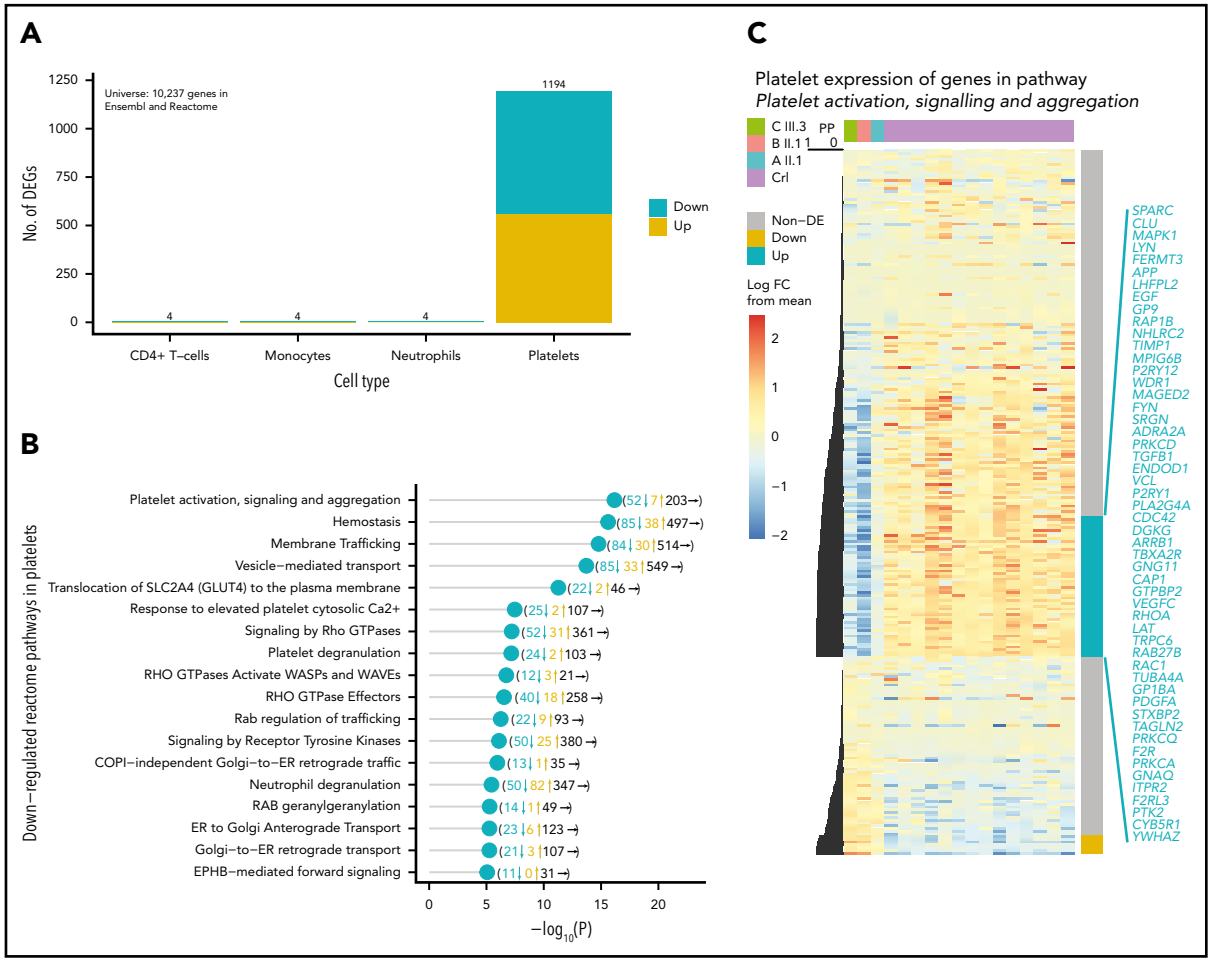

Figure 5. IKZF5 deficiency misregulates transcription in MKs. (A) Barplot of the number of up- and downregulated Reactome/Ensembl coding genes in CD4$^+$ T cells, monocytes, neutrophils, and platelets that are differentially expressed between 14 unrelated controls and 3 unrelated cases. (B) Enriched downregulated pathways in platelets with $P < 10^{-5}$. The number of downregulated, upregulated, and nondifferentially expressed genes in each pathway are shown in brackets. (D) Heatmap of expression for genes in the "platelet activation, signaling, and aggregation" Reactome pathway. The expression levels have been row-normalized such that the color represents the log FC of expression between samples and the mean log expression weighted by the number of cases and controls. The cases are on the left-most 3 columns and the controls are on the right-most 14 columns. The PP of association is shown to the left of the heatmap and the significantly down- (blue) and upregulated (yellow) genes are shown to the right of the heatmap. The significantly downregulated genes are listed in blue. FC, fold change.

cytopenias, or morphological changes on the blood smear) in any of the cases presented here and, unlike the other Ikaros proteins, there is no evidence of lymphoid or immune dysregulation. Therefore, based on the available evidence, thrombocytopenia resulting from rare missense variants in *IKZF5*, is associated with a good prognosis, in sharp contrast with thrombocytopenia from mutations in other TFs such as *RUNX1* and *ETV6*. The reduction in PLT in *IKZF5* cases is mild: none of the PLTs in members of the 5 pedigrees were $<70 \times 10^9$/L and 1 unrecallable carrier had a PLT as high as 184×10^9/L, reflecting the complex regulation of megakaryopoiesis and the ensuing variation in PLT in the normal population. However, there was no evidence of alterations in mean platelet volume in *IKZF5* cases compared with their healthy relatives.

Heterozygous mutations in the DNA-binding Znf domains of *IKZF1* exert a dominant-negative effect,[46,47] with interactions between the WT and mutated DNA-binding domains resulting in dimers that lack transcriptional activity.[48] We propose that the mechanism through which the heterozygous variants in *IKZF5* exert their effect is similar. We have shown that the *IKZF5* variants cause abnormal cellular localization and decreased chromatin binding in HEK293T cells and, in vivo, this would be expected to affect transcription. The discovery of rare missense variants in the N-terminal Znf domains of *IKZF5* as a novel cause of inherited thrombocytopenia highlights an important role for this previously unknown TF in megakaryocyte and platelet biology.

Acknowledgments

The authors thank Ma Hazel Cordial for assisting in patient sampling and Katherine Wedderburn and Lindsay Walker for international sample handling; NIHR BioResource volunteers and their families for their participation, and gratefully acknowledge NIHR BioResource centers and National Health Service (NHS) Trusts and staff for their contribution; and NIHR and NHS Blood and Transplant.

Funding for the project was provided by the NIHR (RG65966). C.L. and M.C.S. received funding from MRC Clinical Research Training Fellowships (MR/J011711/1 and MR/R002363/1). K.F. is supported by the Research Council of the University of Leuven (BOF KU Leuven, Belgium, OT/14/098) and grants from CSL Behring, Bayer, and SOBI. M.F. is supported by the British Heart Foundation (FS/18/53/33863). D.S.'s work

has been supported in part by an Isaac Newton fellowship to M.F. S.S. is the recipient of an NIHR Academic Clinical Fellowship.

The views expressed are those of the author(s) and not necessarily those of the NHS, the NIHR, or the Department of Health.

Authorship

Contribution: E.T., K.F., C.L., and S.S. wrote the manuscript; D.G., D.S., R.J.R., and K.M. edited the manuscript; C.L., S.S., R.F., S.M., K.S., M.J.S., J.-C.B., C.A.-A., K.G., M.A.L., M.S.C. and K.M. enrolled patients and collected clinical data; S.S., C.L., and K.M. coordinated cosegregation studies; S.P. supported project coordination; C.T., M.S., F.B., L.S., J.C.S., M.C.S., S.F., and K.F. performed experiments; W.E. analyzed blood smears; C.J.P. supervised the whole-genome sequencing (WGS) bioinformatics pipeline; K.E.S. managed WGS logistics; D.G., D.S., N.G., L.G., and E.T. performed data analyses; R.J.R. performed structural modelling; and W.H.O., M.L., M.F., K.F., and E.T. supervised the project.

Conflict-of-interest disclosure: The authors have no conflicts of interest to declare.

A complete list of the members of the NIHR BioResource appears in the supplemental appendix.

ORCID profiles: C.L., 0000-0003-0406-4776; S.M., 0000-0001-5364-6241; M.S., 0000-0002-0665-4625; N.G., 0000-0002-1132-1059; K.G., 0000-0002-8934-0700; S.P., 0000-0002-9222-3812; C.J.P., 0000-0003-4006-7261; M.C.S., 0000-0003-4503-0265; L.S., 0000-0002-4352-1151; R.J.R., 0000-0001-8273-0047; K.E.S., 0000-0002-6823-3252; M.A.L., 0000-0002-8268-3268; K.F., 0000-0002-4381-2442; E.T., 0000-0002-1820-6563.

Correspondence: Ernest Turro, University of Cambridge, Department of Haematology, Long Rd, Cambridge CB2 0PT, United Kingdom; e-mail: et341@cam.ac.uk.

Footnotes

Submitted 26 March 2019; accepted 10 June 2019. Prepublished online as *Blood* First Edition paper, 19 June 2019; DOI 10.1182/blood.2019000782.

*C.L., D.G., S.S., and R.F. contributed equally to this study.

†K.F. and E.T. contributed equally to this study.

The RNA-seq data reported in this article have been deposited at the European Genome phenome Archive (accession number ID EGAD00001005107).

The online version of this article contains a data supplement.

There is a *Blood* Commentary on this article in this issue.

The publication costs of this article were defrayed in part by page charge payment. Therefore, and solely to indicate this fact, this article is hereby marked "advertisement" in accordance with 18 USC section 1734.

REFERENCES

1. Noris P, Pecci A. Hereditary thrombocytopenias: a growing list of disorders. *Hematology Am Soc Hematol Educ Program*. 2017;2017:385-399.
2. Lentaigne C, Freson K, Laffan MA, Turro E, Ouwehand WH; BRIDGE-BPD Consortium and the ThromboGenomics Consortium. Inherited platelet disorders: toward DNA-based diagnosis. *Blood*. 2016;127(23):2814-2823.
3. Song WJ, Sullivan MG, Legare RD, et al. Haploinsufficiency of CBFA2 causes familial thrombocytopenia with propensity to develop acute myelogenous leukaemia. *Nat Genet*. 1999;23(2):166-175.
4. Zhang MY, Churpek JE, Keel SB, et al. Germline ETV6 mutations in familial thrombocytopenia and hematologic malignancy. *Nat Genet*. 2015;47(2):180-185.
5. Thompson AA, Nguyen LT. Amegakaryocytic thrombocytopenia and radio-ulnar synostosis are associated with HOXA11 mutation. *Nat Genet*. 2000;26(4):397-398.
6. Niihori T, Ouchi-Uchiyama M, Sasahara Y, et al. Mutations in MECOM, encoding oncoprotein EVI1, cause radioulnar synostosis with amegakaryocytic thrombocytopenia. *Am J Hum Genet*. 2015;97(6):848-854.
7. Freson K, Wijgaerts A, Van Geet C. GATA1 gene variants associated with thrombocytopenia and anemia. *Platelets*. 2017;28(7):731-734.
8. Raslova H, Komura E, Le Couédic JP, et al. FLI1 monoallelic expression combined with its hemizygous loss underlies Paris-Trousseau/Jacobsen thrombopenia. *J Clin Invest*. 2004;114(1):77-84.
9. Georgopoulos K, Winandy S, Avitahl N. The role of the Ikaros gene in lymphocyte development and homeostasis. *Annu Rev Immunol*. 1997;15(1):155-176.
10. Boutboul D, Kuehn HS, Van de Wyngaert Z, et al. Dominant-negative IKZF1 mutations cause a T, B, and myeloid cell combined immunodeficiency. *J Clin Invest*. 2018;128(7):3071-3087.
11. John LB, Ward AC. The Ikaros gene family: transcriptional regulators of hematopoiesis and immunity. *Mol Immunol*. 2011;48(9-10):1272-1278.
12. Kamihara J, Shimamura A. It's ALL in the family: IKZF1 and hereditary leukemia. *Cancer Cell*. 2018;33(5):798-800.
13. Chen L, Kostadima M, Martens JHA, et al. Transcriptional diversity during lineage commitment of human blood progenitors. *Science*. 2014;345(6204):1251033.
14. Perdomo J, Holmes M, Chong B, Crossley M. Eos and pegasus, two members of the Ikaros family of proteins with distinct DNA binding activities. *J Biol Chem*. 2000;275(49):38347-38354.
15. Fan Y, Lu D. The Ikaros family of zinc-finger proteins. *Acta Pharm Sin B*. 2016;6(6):513-521.
16. The NIHR BioResource on behalf of the 100,000 Genomes Project. Whole-genome sequencing of rare disease patients in a national healthcare system. *bioRxiv*. Preprint.
17. Westbury SK, Turro E, Greene D, et al; BRIDGE-BPD Consortium. Human phenotype ontology annotation and cluster analysis to unravel genetic defects in 707 cases with unexplained bleeding and platelet disorders. *Genome Med*. 2015;7(1):36.
18. Korbie DJ, Mattick JS. Touchdown PCR for increased specificity and sensitivity in PCR amplification. *Nat Protoc*. 2008;3(9):1452-1456.
19. Greene D, Richardson S, Turro E; NIHR BioResource. A fast association test for identifying pathogenic variants involved in rare diseases. *Am J Hum Genet*. 2017;101(1):104-114.
20. Freson K, Devriendt K, Matthijs G, et al. Platelet characteristics in patients with X-linked macrothrombocytopenia because of a novel GATA1 mutation. *Blood*. 2001;98(1):85-92.
21. Wijgaerts A, Wittevrongel C, Thys C, et al. The transcription factor GATA1 regulates NBEAL2 expression through a long-distance enhancer. *Haematologica*. 2017;102(4):695-706.
22. Brunet JG, Iyer JK, Badin MS, et al. Electron microscopy examination of platelet whole mount preparations to quantitate platelet dense granule numbers: Implications for diagnosing suspected platelet function disorders due to dense granule deficiency. *Int J Lab Hematol*. 2018;40(4):400-407.
23. Suzek BE, Wang Y, Huang H, McGarvey PB, Wu CH; UniProt Consortium. UniRef clusters: a comprehensive and scalable alternative for improving sequence similarity searches. *Bioinformatics*. 2015;31(6):926-932.
24. McNicholas S, Potterton E, Wilson KS, Noble ME. Presenting your structures: the CCP4mg molecular-graphics software. *Acta Crystallogr D Biol Crystallogr*. 2011;67(Pt 4):386-394.
25. Petersen R, Lambourne JJ, Javierre BM, et al. Platelet function is modified by common sequence variation in megakaryocyte super enhancers. *Nat Commun*. 2017;8(1):16058.

26. Cunningham F, Achuthan P, Akanni W, et al. Ensembl 2019. *Nucleic Acids Res*. 2019; 47(D1):D745-D751.

27. Langmead B, Trapnell C, Pop M, Salzberg SL. Ultrafast and memory-efficient alignment of short DNA sequences to the human genome. *Genome Biol*. 2009;10(3):R25.

28. Turro E, Su SY, Gonçalves Â, Coin LJ, Richardson S, Lewin A. Haplotype and isoform specific expression estimation using multi-mapping RNA-seq reads. *Genome Biol*. 2011; 12(2):R13.

29. Turro E, Astle WJ, Tavaré S. Flexible analysis of RNA-seq data using mixed effects models. *Bioinformatics*. 2014;30(2):180-188.

30. Yu G, He QY. ReactomePA: an R/Bioconductor package for reactome pathway analysis and visualization. *Mol Biosyst*. 2016; 12(2):477-479.

31. Ashkenazy H, Abadi S, Martz E, et al. ConSurf 2016: an improved methodology to estimate and visualize evolutionary conservation in macromolecules. *Nucleic Acids Res*. 2016; 44(W1):W344-W350.

32. Di Angelantonio E, Thompson SG, Kaptoge S, et al; INTERVAL Trial Group. Efficiency and safety of varying the frequency of whole blood donation (INTERVAL): a randomised trial of 45 000 donors. *Lancet*. 2017;390(10110): 2360-2371.

33. Hashimoto H, Wang D, Horton JR, Zhang X, Corces VG, Cheng X. Structural basis for the versatile and methylation-dependent binding of CTCF to DNA. *Mol Cell*. 2017;66(5): 711-720.

34. Hashimoto H, Zhang X, Zheng Y, Wilson GG, Cheng X. Denys-Drash syndrome associated WT1 glutamine 369 mutants have altered sequence-preferences and altered responses to epigenetic modifications. *Nucleic Acids Res*. 2016;44(21):10165-10176.

35. Jacobs GH. Determination of the base recognition positions of zinc fingers from sequence analysis. *EMBO J*. 1992;11(12): 4507-4517.

36. Wuttke DS, Foster MP, Case DA, Gottesfeld JM, Wright PE. Solution structure of the first three zinc fingers of TFIIIA bound to the cognate DNA sequence: determinants of affinity and sequence specificity. *J Mol Biol*. 1997;273(1):183-206.

37. Dovat S, Ronni T, Russell D, Ferrini R, Cobb BS, Smale ST. A common mechanism for mitotic inactivation of C2H2 zinc finger DNA-binding domains. *Genes Dev*. 2002;16(23):2985-2990.

38. Altschul SF, Gish W, Miller W, Myers EW, Lipman DJ. Basic local alignment search tool. *J Mol Biol*. 1990;215(3):403-410.

39. Fabregat A, Jupe S, Matthews L, et al. The Reactome Pathway Knowledgebase. *Nucleic Acids Res*. 2018;46(D1):D649-D655.

40. White JG. Ultrastructural studies of the gray platelet syndrome. *Am J Pathol*. 1979;95(2): 445-462.

41. Albers CA, Cvejic A, Favier R, et al. Exome sequencing identifies NBEAL2 as the causative gene for gray platelet syndrome. *Nat Genet*. 2011;43(8):735-737.

42. Monteferrario D, Bolar NA, Marneth AE, et al. A dominant-negative GFI1B mutation in the gray platelet syndrome. *N Engl J Med*. 2014; 370(3):245-253.

43. Favier R, Jondeau K, Boutard P, et al. Paris-Trousseau syndrome: clinical, hematological, molecular data of ten new cases. *Thromb Haemost*. 2003;90(5):893-897.

44. Aneja K, Jalagadugula G, Mao G, Singh A, Rao AK. Mechanism of platelet factor 4 (PF4) deficiency with RUNX1 haplodeficiency: RUNX1 is a transcriptional regulator of PF4. *J Thromb Haemost*. 2011;9(2):383-391.

45. Gunay-Aygun M, Zivony-Elboum Y, Gumruk F, et al. Gray platelet syndrome: natural history of a large patient cohort and locus assignment to chromosome 3p. *Blood*. 2010;116(23): 4990-5001.

46. Winandy S, Wu P, Georgopoulos K. A dominant mutation in the Ikaros gene leads to rapid development of leukemia and lymphoma. *Cell*. 1995;83(2):289-299.

47. Sun L, Crotty ML, Sensel M, et al. Expression of dominant-negative Ikaros isoforms in T-cell acute lymphoblastic leukemia. *Clin Cancer Res*. 1999;5(8):2112-2120.

48. Sun L, Liu A, Georgopoulos K. Zinc finger-mediated protein interactions modulate Ikaros activity, a molecular control of lymphocyte development. *EMBO J*. 1996;15(19): 5358-5369.